

# Sterol uptake and sterol biosynthesis act coordinately to mediate antifungal resistance in *Candida glabrata* under azole and hypoxic stress

QINGDI QUENTIN LI<sup>1</sup>, HUEI-FUNG TSAI<sup>1</sup>, AJEET MANDAL<sup>2</sup>, BRYAN A. WALKER<sup>1</sup>,  
JASON A. NOBLE<sup>1</sup>, YUICHI FUKUDA<sup>1</sup> and JOHN E. BENNETT<sup>1</sup>

<sup>1</sup>Clinical Mycology Section, Laboratory of Clinical Infectious Diseases, National Institute of Allergy and Infectious Diseases; <sup>2</sup>Molecular and Cellular Biochemistry Section, National Institute of Dental and Craniofacial Research, National Institutes of Health, Bethesda, MD 20892, USA

Received October 11, 2017; Accepted February 23, 2018

DOI: 10.3892/mmr.2018.8716

**Abstract.** Pathogenic fungi, including *Candida glabrata*, develop strategies to grow and survive both *in vitro* and *in vivo* under azole stress. However, the mechanisms by which yeast cells counteract the inhibitory effects of azoles are not completely understood. In the current study, it was demonstrated that the expression of the ergosterol biosynthetic genes *ERG2*, *ERG3*, *ERG4*, *ERG10*, and *ERG11* was significantly upregulated in *C. glabrata* following fluconazole treatment. Inhibiting ergosterol biosynthesis using fluconazole also increased the expression of the sterol influx transporter *AUS1* and the sterol metabolism regulators *SUT1* and *UPC2* in fungal cells. The microarray study quantified 35 genes with elevated mRNA levels, including *AUS1*, *TIR3*, *UPC2*, and 8 *ERG* genes, in a *C. glabrata* mutant strain lacking *ERG1*, indicating that sterol importing activity is increased to compensate for defective sterol biosynthesis in cells. Bioinformatic analyses further revealed that those differentially expressed genes were involved in multiple cellular processes and biological functions, such as sterol biosynthesis, lipid localization, and sterol transport. Finally, to assess whether sterol uptake affects yeast susceptibility to azoles, we generated a *C. glabrata aus1Δ* mutant strain. It was shown that loss of *Aus1p* in *C. glabrata* sensitized the pathogen to azoles and enhanced the efficacy of drug exposure under low oxygen tension. In contrast, the presence of exogenous cholesterol or ergosterol in medium rendered the *C. glabrata AUS1* wild-type strain highly resistant

to fluconazole and voriconazole, suggesting that the sterol importing mechanism is augmented when ergosterol biosynthesis is suppressed in the cell, thus allowing *C. glabrata* to survive under azole pressure. On the basis of these results, it was concluded that sterol uptake and sterol biosynthesis may act coordinately and collaboratively to sustain growth and to mediate antifungal resistance in *C. glabrata* through dynamic gene expression in response to azole stress and environmental challenges.

## Introduction

*Candida* species are ubiquitous fungi and the most common fungal pathogens affecting humans. *Candida*, in particular, affects high-risk patients who are either immunocompromised or critically ill. More than 100 species of *Candida* exist, but only a few are recognized as causing disease in humans. *Candida glabrata* and *Candida albicans* account for 70 to 80% of yeasts isolated from patients with invasive candidiasis. In recent decades, *C. glabrata* has become important because of its increasing world-wide incidence and because of its developing resistance to antifungals, including azoles, in the clinic.

Azole antifungal agents such as fluconazole and voriconazole are approved therapy for candidemia and invasive candidiasis caused by *C. glabrata* (1). Mechanisms of azole resistance include i) increased drug export (efflux pumps), ii) lost drug targets (e.g., altered drug target binding site), iii) up-regulated homeostatic stress-response pathways to deal with azole-associated damage, and iv) changed biosynthetic pathways (particularly sterol synthesis) that circumvent or attenuate the effects of azole inhibition (2).

The cellular toxicity of azole antifungals occurs primarily through their ability to affect the fungal cell membrane by inhibiting the biosynthesis of ergosterol, the principal sterol in the fungal cell membrane, leading to the depletion of ergosterol and an accumulation of possibly toxic sterol intermediates in the cytoplasmic membrane. Azole antifungal compounds (imidazoles and triazoles) inhibit cytochrome P-450 dependent sterol 14 $\alpha$ -demethylase (Erg11p), an enzyme that catalyzes the oxidative removal of the 14 $\alpha$ -methyl group of lanosterol in

---

*Correspondence to:* Dr Qingdi Quentin Li or Dr John E. Bennett, Clinical Mycology Section, Laboratory of Clinical Infectious Diseases, National Institute of Allergy and Infectious Diseases, National Institutes of Health, 9000 Rockville Pike, Bethesda, MD 20892, USA

E-mail: quentin.li@nih.gov

E-mail: jbenett@niaid.nih.gov

**Key words:** *Candida glabrata*, azole resistance, fluconazole, voriconazole, ergosterol synthesis, sterol uptake

the ergosterol biosynthetic pathway (2). Fungal cells exposed to azoles must either synthesize more endogenous ergosterol or import exogenous sterol if they are to survive antimycotic treatment.

Sterol uptake appears to confer resistance to antifungal drugs since mutant strains of *Candida* species lacking *AUS1* and *TIR3*, the sterol influx transporters (3), or *UPC2*, the transcription factor that controls *AUS1* and *TIR3* expression (3-5), exhibit reduced uptake of cholesterol and are hypersensitive to azoles (6,7), whereas enhanced *UPC2* or *AUS1* expression and cholesterol uptake have been implicated in the azole-resistant phenotype (6,7). Furthermore, several studies have even suggested that pathogenic fungi can scavenge free sterols for the cell membrane, including cholesterol, resulting in resistance to polyene and azole antifungals (8). Increased uptake of exogenous cholesterol may be associated with drug resistance in clinical isolates of bile-dependent *C. glabrata* cells as well as in sterol auxotrophic *C. glabrata* strains (9). These observations indicate that the ability to scavenge exogenous sterols, when ergosterol biosynthesis is defective or is blocked by antimycotic agents, may play an important role in increased azole resistance in pathogenic fungal species.

Besides sterol uptake, alteration in sterol biosynthesis seems to also affect fungal susceptibility to antifungals. *ERG11* is one of the critical genes in the ergosterol biosynthetic pathway, and its encoding protein product Erg11p (or CYP51p depending on nomenclature) is the major target enzyme of azole antifungals. Mutations in *ERG11* are the most common mechanism of azole resistance in *C. albicans* (10). Over-expression of *ERG11* has been attributed to decreases in azole activity in *C. albicans*. Alterations in other enzymes of the ergosterol biosynthetic pathway, particularly *ERG3* (C-5 sterol desaturase), *ERG5* (C-22 sterol desaturase), *ERG6* (C-24 sterol methyl-transferase), and *ERG25* (C-4 sterol methyl-oxidase), which are up-regulated with inhibition of Erg11p, have also been documented to reduce azole susceptibility of *C. albicans*. In *C. glabrata*, depletion of the ergosterol content in a *CgERG1* mutant increases the levels of susceptibility to azoles, while complementation of the *CgERG1* mutation restores drug sensitivity to wild-type levels (8). In both *C. albicans* and *C. glabrata*, regulation of sterol synthesis is vital to azole susceptibility.

In this study, we assessed the role of two protective mechanisms in conferring antifungal susceptibility in *C. glabrata*. We showed that expression of the genes involved in both sterol uptake and sterol synthesis is up-regulated in *C. glabrata* when ergosterol is depleted by azole treatment and when ergosterol biosynthesis is defective. We further corroborated that pathogenic fungi can accumulate exogenous sterols from the environment as a protective strategy to survive under azole and hypoxic stress. These findings suggest that sterol uptake and sterol synthesis may act coordinately and collaboratively to sustain growth and to mediate antifungal tolerance in *C. glabrata* through dynamic gene expression in response to azole pressure and environmental changes.

## Materials and methods

**Cell culture and drug treatment.** All *C. glabrata* strains (Table I) used in the present study were cultured on YPD agar

containing 1% Bacto yeast extract (Difco Laboratories, Detroit, MI, USA), 2% Bacto peptone (Difco Laboratories), and 2% glucose (Sigma-Aldrich, St. Louis, MO, USA). NCCLS84, CgI660, CgTn201S, and CgTn201Su/aus1 were also grown on minimal (MIN) agar containing 0.67% Yeast Nitrogen Base without amino acids (Difco Laboratories) plus 2% glucose. The *ura3* mutants Cg84u, CgI660u, and CgTn201Su were grown in MIN medium supplemented with 20  $\mu$ g/ml of uracil (Sigma-Aldrich) or were selected on a MIN plus uracil agar plate containing 0.1% 5-fluoroorotic acid (FOA) (Lancaster, Pelham, NH, USA). YEPG agar was used for drug sensitivity assay, which contained 1% Bacto yeast extract (Difco Laboratories), 2% Bacto peptone (Difco Laboratories), 3% glycerol (Invitrogen/Life Technologies, Carlsbad, CA, USA), 1% ethanol (Warner-Graham, Inc., Cockeysville, MD), and 2% agar (Difco Laboratories).

Fluconazole (Euroasian Chemicals Private Ltd., Mumbai, India) was added to cultures of each strain at a final concentration of 200  $\mu$ g/ml, followed by continued incubation with shaking for 2 h. Cell cultures without fluconazole treatment served as controls. After incubation, the cells were harvested, and the cell pellets were stored at -80°C until the subsequent isolation of RNA.

The BBL GasPak Plus gas generator envelope (Becton Dickinson Microbiology Systems, Sparks, MD, USA) or the BBL GasPak Pouch Anaerobic Systems (Becton Dickinson Microbiology Systems, Cockeysville, MD, USA) was used for cultures grown under conditions of low oxygen tension (hypoxia). To mimic the host environment of animals and humans, *C. glabrata* cells were also grown in the presence of 5% CO<sub>2</sub> under low oxygen conditions using an InvivoO2 400 workstation at 37°C with shaking at 200 rpm (Ruskin Technology Ltd., Bridgend, UK). For analysis of sterol uptake and exogenous sterol utilization, 2 mg of ergosterol or cholesterol was dissolved in a mixture of 50% ethanol and 50% Tween-80 (Sigma-Aldrich) to give a 2 mg/ml stock solution, which was used to supplement the media with a final sterol concentration of 20  $\mu$ g/ml. For comparison, the same final concentration of ethanol-Tween-80 without sterol was used.

**Drug sensitivity assay.** The susceptibility of the *C. glabrata* strains CgI660, CgTn201S, and CgTn201Su/aus1 to fluconazole and voriconazole was determined on MIN and YEPG agar media using an E-test (AB Biodisk, Solna, Sweden) according to the manufacturer's instructions. In brief, logarithmic-phase cells were harvested and adjusted to the desired concentrations by counting the number of cells with a hemocytometer. From each cell suspension, 200  $\mu$ l (1x10<sup>6</sup> cells/ml) was plated in duplicate on MIN and YEPG agar. All plates were incubated under conditions of low oxygen tension at 37°C for 3 days. Growth inhibition zones (minimum inhibitory concentration, MIC) to fluconazole and voriconazole were measured.

**RT-qPCR analysis.** Total RNA was extracted from *C. glabrata* (Cg84u) logarithmic-phase cultures grown in YPD broth using TRIzol reagent (Invitrogen; Thermo Fisher Scientific, Inc., Waltham, MA, USA) according to the manufacturer's instructions. RNA was converted to cDNA using the High Capacity cDNA Reverse Transcription kit (Applied Biosystems; Thermo Fisher Scientific, Inc.) as previously described (11). Primers

and probes were designed in our laboratory using the primer analysis software Primer Express 3.0 (Applied Biosystems; Thermo Fisher Scientific, Inc.). TaqMan probes were synthesized by Applied Biosystems (Thermo Fisher Scientific, Inc.) and primers were synthesized by Invitrogen (Thermo Fisher Scientific, Inc.). The sequences of TaqMan probes and forward and reverse primers, as well as the gene numbers for all genes assessed in this study, are listed in Table II. To study gene expression, the amplification was detected in real time using both SYBR Green chemistry (SYBR-Green PCR Master Mix; Applied Biosystems; Thermo Fisher Scientific, Inc.) and TaqMan chemistry (TaqMan Universal PCR Master Mix; Applied Biosystems; Thermo Fisher Scientific, Inc.) as described previously (11).

**Microarray hybridization and data analysis.** DNA microarray analysis was used to identify genes with altered expression in the *C. glabrata erg1* mutant strain CgTn201S and the wild-type strain Cg1660. Total RNA was isolated from the log phase culture of *C. glabrata* grown in YPD by using TRIzol (Invitrogen; Thermo Fisher Scientific, Inc.) and the RNeasy MiniElute Cleanup kit (Qiagen, Valencia, CA, USA). RNA was assessed for quality using the Agilent 2100 Bioanalyzer with the RNA 6000 Nano Reagent Kit. Pin-spotted 70-mer oligonucleotide in-house arrays fabricated at the National Institute of Allergy and Infectious Diseases (NIAID) were used for analysis of the pair strains. In brief, a total of 5,908 70-mer oligonucleotides were purchased from Institut Pasteur (Paris, France) and were used for microarray printing at the NIAID Microarray Research Facility. Expression of each open reading frame (ORF) was measured by hybridization to a specific 70-mer oligonucleotide. Thirty micrograms of total RNA from the *erg1* mutant strain CgTn201S and the wild-type strain Cg1660 was reverse-transcribed to cDNA to incorporate the fluorescent Cy3-dUTP and Cy5-dUTP (GE Healthcare, Piscataway, NJ, USA), respectively. The labeled cDNA of the paired mutant/wild-type strain was combined and used for microarray hybridization. Six microarrays were performed for analysis of the *erg1* mutant/wild-type pair, including two with reciprocal labeling. The microarrays were prehybridized at 42°C in prehybridization buffer [5 x SSC (1 x SSC is 0.15 M NaCl plus 0.015 M sodium citrate), 1% bovine serum albumin (BSA), 0.1% SDS] for 30 to 60 min and then hybridized to the labeled cDNA in 50 µl of hybridization buffer [25% formamide, 5 x SSC, 0.2% SDS, 20 µg/ml poly (dA)<sub>40-60</sub>, 200 µg/ml Cot-1 DNA (Invitrogen; Thermo Fisher Scientific, Inc.), 80 µg/ml yeast tRNA] overnight at 42°C. The microarrays were washed three times in wash buffer A (1 x SSC, 0.05% SDS) and wash buffer B (0.1 x SSC). The in-house arrays were scanned with a GenePix 4000B scanner (Molecular Devices, Sunnyvale, CA, USA). All microarray data archive and statistical calculations were performed on the 'processed signal' data by using the Web-based mAdb analysis system provided by the Bioinformatics and Molecular Analysis group (BIMAS) at the Center for Information Technology (CIT), National Institutes of Health. The data were filtered with the parameters that included genes present in four or more arrays and each array with 80% or more genes present. The data set of the paired strains was then analyzed by Student's t-test. The

genes with P-values less than 0.001 and with at least 1.5-fold altered gene expression were then selected. The final data set included all genes with altered expression in the pair.

**Cloning of CgAUS1.** The full nucleotide sequence of the *C. glabrata AUS1* homolog (*CgAUS1*) was obtained from the Candida Genome Database ([www.candidagenome.org](http://www.candidagenome.org)). A 1,087 bp partial ORF of the *CgAUS1* gene was obtained by PCR with PfuUltra High-Fidelity DNA polymerase (Stratagene, La Jolla, California, USA), primer set CgAUS1S (5'-TTGAAGTTGCCTCTTGACTC-3') and CgAUS1AS (5'-AAGGCAACAAACACAGCGGCAG-3'), and the total genomic DNA of Cg1660 was used as the template. The PCR parameters were 2 min at 95°C, followed by 30 cycles of 95°C for 30 sec, 53°C or 55°C for 30 sec, and 72°C for 1 min 30 sec, and then extended at 72°C for 10 min. The 1,087 bp PCR product, which was used as a probe for Southern blotting, was then cloned into pCR-Blunt II-TOPO (Invitrogen; Thermo Fisher Scientific, Inc.) to produce plasmid pCgAUS1.

**Construction of the Candida glabrata Cgerg1 and Cgaus1A double mutant.** The *Cgerg1* mutant was generated in our laboratory as described previously (8). Gene deletion of *Cgaus1* was performed as described by Vermitsky *et al* (12). Briefly, the primer pair CgAUS1D1S (TTGAAATTCTCGGAAAGA AACATCAAATCAAAAAATTTTAACCTTCTAAAACCTT GTTCTTTTTTTGGGAAATATAAGATGTGCGAAAGCTA CATATAAGGA) and CgAUS1D2AS (AGTAGATTAAG AAAAGTGTAAATTTAAGAATAAAATGGAATTGTTA TTTCATTAAGCTTGTAGGAGTCACTCTTATTAGT TTTGCTGGCCGCATCT) was used to generate the *CgAUS1* deletion cassette using YEP24 as the template to amplify *Saccharomyces cerevisiae URA3*, which served as the selection marker. An additional round of PCR using the primer pair CgAUS1D3S (CCCCAACTATCAATTTTCTTTAAATCA AGGAAAATCTATTACATTCGCTATTAATCTCTACTA TCTTTATCTTAGTTTTTTGAAATTCTCGGAAAGAAAC) and CgAUS1D4AS (ATTATATTTTAAATTTTGTGTAT AGCTTTTTTGCTGTAAAGGTGAAAAACCGGGAATT TTGAGCATTAGTATTAGTAGATTAAAGAAAAGTGTT AAAT) extended the 5' and 3' ends with about a 160 bp homologous region on each end of the *CgAUS1* deletion cassettes to increase the efficiency of homologous recombination. *S. cerevisiae URA3* was transformed into CgTn201Su (*Cgura3 Cgerg1::Tn5<Cm ura3>*) to construct the *Cgerg1/aus1* double mutant CgTn201Su/aus1 via a successful double cross-over homologous recombination, which resulted in replacement of the *CgAUS1* ORF with *S. cerevisiae URA3* (Fig. 1A). The *CgERG1* locus in the clinical isolate Cg1660 and its transposon mutant CgTn201S (*Cgerg1*) are shown in Fig. 1B. Transformants were selected on MIN medium, and the deletion of *CgAUS1* was confirmed by Southern blot analysis of the EcoRI-digested genomic DNA (Fig. 1C). The purified 1.2-kb *ScURA3* probe detected a single signal in the *Cgerg1* mutant CgTn201S; two signals were detected in the two putative *Cgerg1/aus1* mutants CgTn201Su/aus1-1 and CgTn201Su/aus1-2, while there was no signal in the parental strain Cg1660 (Fig. 1C, right panel). The 1087-bp *CgAUS1* probe detected a single 6.3-kb signal in Cg1660 and CgTn201S, but not in the two putative *Cgerg1/aus1*

Table I. *Candida glabrata* strains used in this study.

Strain	Parental strain	Genotype or description	Reference or source
NCCLS84		Wild-type (ATCC90030) <sup>a</sup>	ATCC <sup>a</sup>
Cg84u	NCCLS84	<i>Cgura3</i>	(8)
Cg1660		Clinical isolate	FHCRC <sup>b</sup>
Cg1660u	Cg1660	<i>Cgura3</i>	(8)
CgTn201S	Cg1660u	<i>Cgura3 Cgergl::Tn5&lt;Cm URA3&gt;</i>	(8)
CgTn201Su	CgTn201S	<i>Cgura3 Cgergl::Tn5&lt;Cm ura3&gt;</i>	Present study
CgTn201Su/aus1	CgTn201Su	<i>Cgura3 Cgergl::Tn5&lt;Cm ura3&gt;</i> <i>Cgaus1Δ::URA3</i>	Present study

<sup>a</sup>American Type Culture Collection (ATCC), Manassas, VA, USA. <sup>b</sup>FHCRC, Fred Hutchinson Cancer Research Center, Seattle, WA, USA.

Table II. Primers and TaqMan probes for RT-qPCR analysis of gene expression used in this study.

Gene	Primer and probe sequence (5'→3')	Gene number <sup>a</sup>
<i>ACT1</i>		
F	TTGGACTCTGGTGACGGTGTTA	CAGL0K12694g
R	AAAATAGCGTGTGGCAAAGAGAA	
P	CCACGTTGTTCCAATTTACGCCGG	
<i>RDN5.8</i>		
F	CTTGTTCTCGCATCGATGA	CAGL0L13387r
R	GGCGCAATGTGCGTTCA	
P	ACGCAGCGAAATGCGATACGTAATGTG	
<i>ERG2</i>		
F	TCCCAGGTATGACCCATCATC	CAGL0L10714g
R	TGCGAAGGAGTTTTGATCCAT	
P	ACAAAAGGGCTACGCAAAGCAATACGC	
<i>ERG3</i>		
F	TGCACTGGCCTCGTGTCTAC	CAGL0F01793g
R	TAACCGTCGACTGGGTGGAA	
P	TGGTTGGTCTGCACTCCATTCGCC	
<i>ERG4</i>		
F	CCCTCAATTAGGTGTCGTCATGT	CAGL0A00429g
R	GGCACGATTAATTCTTCACCCTTA	
P	CCACTGGCTGTACGCTAACGCTTGTG	
<i>ERG10</i>		
F	GCCAGAACCCCAATTGGTT	CAGL0L12364g
R	TGCAATGACACCTAGGTCAACAG	
P	TTCCAAGGTGCGTTGGCCTCCA	
<i>ERG11</i>		
F	TGTCTTGATGGGTGGTCAACA	CAGL0E04334g
R	CTGGTCTTTCAGCCAAATGCA	
P	CTTCCGCTGCTACCTCCGCTTGG	
<i>PDR16</i>		
F	CCTGGAGACGTGAATTTGGAAT	CAGL0J07436g
R	ACAGCAACCAAATCCGATGTAA	
P	CTCGTCACCATTTTCTTCACCCAAATGG	
<i>PDR16</i>		
F	TTGGCCTGGAGACGTGAATT	CAGL0J07436g
R	GTTTACCACTTTCATTCTCTACAGCAA	
P	TTGGGTGAAGAAAATGGTGACGAGGTTACA	

Table II. Continued.

Gene	Primer and probe sequence (5'→3')	Gene number <sup>a</sup>
<i>AUS1</i>		
F	CCAAGCCACTGCAGGTGAA	CAGL0F01419g
R	GGCGTGAAACAGGGACTTGA	
P	CGGTGCCCAACGTCGGGTATC	
<i>SUT1</i>		
F	GTTGATGGCATTACATGGCAAT	CAGL0I04246g
R	AGTAAAGGAGTTGGATGATGAGTGAA	
P	ACCAATTCCTATCGCCTCCAATGCCA	
<i>SUT2</i>		
F	AGGGCCTTCAAGGTATCGAAGT	CAGL0L09383g
R	TCGGTTTTTGGATCACACCAA	
P	TTGCCTCTCCAAAACAGAACTACCCTCCC	
<i>ECM22</i>		
F	CAATTACAAGAGCATGCAAACATTG	CAGL0C01199g
R	GGAGTTAGCCTGACCATGAGTATTATT	
P	TGCATCAGAAACAGCATATCCAACGACTGT	
<i>UPC2A</i>		
F	AAAATAGTACAGGAGCAACGGAGACT	CAGL0C01199g
R	TGGTTGCACCTGGAGATGAA	
P	CTGTCGCCTTCTCTGAATCTGCTTACACCC	
<i>UPC2B</i>		
F	GGTCGCAAGTGCATTGTTGT	CAGL0F07865g
R	TCAGTCGCATTTGATGTATCTTTAGG	
P	CGTGAATAATCACGATCCTCACATGCA	

<sup>a</sup>Candida Genome Database ([www.candidagenome.org](http://www.candidagenome.org)). F, forward primer; R, reverse primer; P, TaqMan probe, labeled as 5'-FAM, 3'-TAMRA; RT-qPCR, reverse transcription-quantitative polymerase chain reaction.

mutants CgTn201Su/aus1-1 and CgTn201Su/aus1-2 (Fig. 1C, left panel).

**Southern blot analysis.** *Candida glabrata* genomic DNA was isolated from cultures grown in YPD overnight by using the MasterPure Yeast Purification Kit (Epicentre, Madison, WI, USA). Purified DNA fragments were recovered using the Strataprep Gel DNA Extraction kit (Stratagene; Agilent Technologies, Inc., Santa Clara, CA, USA). Hybond-N nylon membranes (Amersham, Arlington Heights, IL, USA) were used for Southern hybridization analyses. DNA probes were labeled with [ $\alpha$ -<sup>32</sup>P] dCTP or [ $\alpha$ -<sup>32</sup>P] dATP (MP Biomedical, Solon, OH, USA) by using the Prime-It II kit (Stratagene; Agilent Technologies, Inc.). DNA cloning and hybridization analyses were done according to the standard protocol.

**Other techniques and reagents.** DNA sequencing was done using the DNA sequencing kit with a dRhodamine dye terminator (Applied Biosystems; Thermo Fisher Scientific, Inc.) and an ABI automatic DNA sequencing system (Perkin-Elmer, Foster City, CA, USA). For sequencing of PCR products, PfuUltra DNA polymerase (Stratagene; Agilent Technologies, Inc.) was used for PCR amplification to minimize the rate of

PCR-introduced mutations. The PCR products were cleaned with the Strataprep PCR Purification kit (Stratagene; Agilent Technologies, Inc.) and were used as templates for DNA sequencing.

**Bioinformatic and statistical analysis.** The Gene Ontology (GO) enrichment analysis and the network visualization of the biological functions related to the differentially expressed genes were performed using Cytoscape software with associated plug-ins (13). To create a functional network by selecting the ClueGO: Function, GO: Biological process, all the network evidence and only the terms with various levels of significance ( $P < 0.1 - < 0.0005$ ) were taken into consideration using the plug-in ClueGO (14), which was followed by enrichment of the functional network with the plug-in CluePedia (15).

Results of RT-qPCR for each gene are presented as the fold-change over the expression in the sample not treated with fluconazole, which was set as 1. The difference in triplicate  $C_q$  values ( $\Delta C_q$ ) was used to calculate the difference between untreated andazole-treated samples. Student's t-test was used to analyze the statistical significance of differences between untreated and fluconazole-treated *C. glabrata* cells, and P-values were adjusted using Holm's

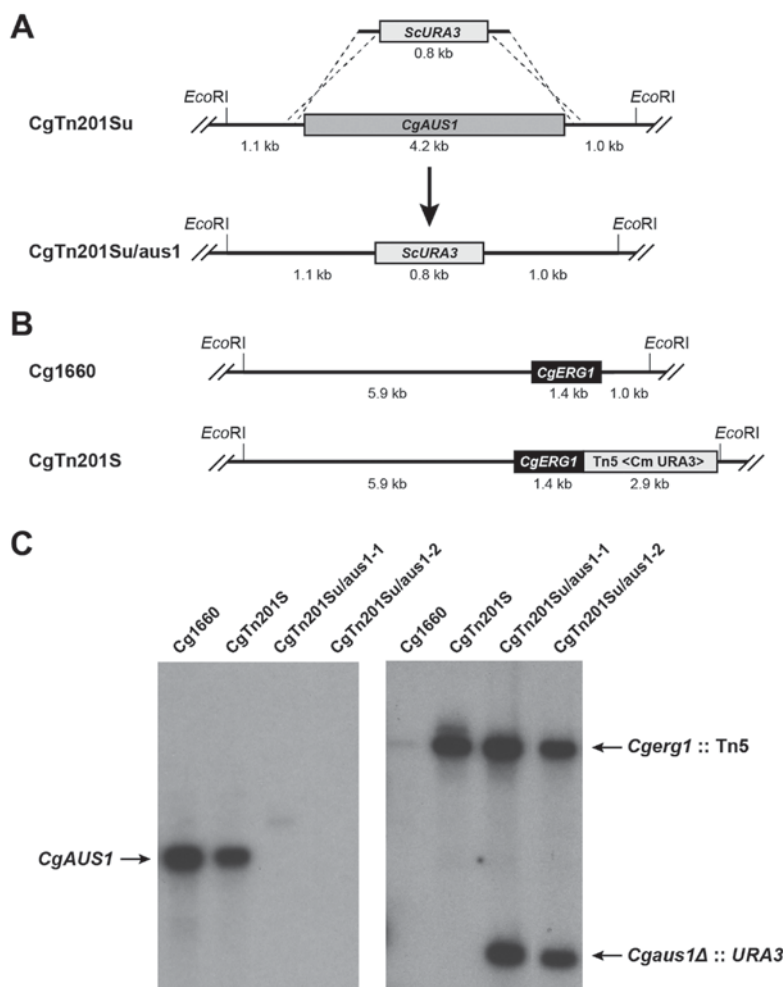


Figure 1. Southern hybridization analysis confirms the deletion and targeted gene replacement of *CgAUS1* in *Candida glabrata*. (A) Deletion strategy of *CgAUS1* in the strain CgTn201Su (*Cgerg1/ura3*). The *CgAUS1* ORF was replaced with *ScURA3* in the mutant CgTn201Su/aus1 (*Cgerg1 Cgaus1Δ*). (B) The *CgERG1* locus in the clinical isolate Cg1660 and its transposon mutant CgTn201S (*Cgerg1*). (C) Southern blot analysis. The genomic DNAs of Cg1660, CgTn201S, and the mutant CgTn201Su/aus1 were digested with *EcoRI*, electrophoresed, and blotted onto a nylon membrane. The membrane was hybridized with the 1087-bp *CgAUS1* probe (left panel) or 1.2-kb *ScURA3* probe (right panel). Lanes (from the left): 1. Cg1660, clinical isolate; 2. CgTn201S, *Cgerg1* mutant; 3. and 4. CgTn201Su/aus1, *Cgerg1 Cgaus1Δ* double mutant. The detected signals for *CgAUS1* (left panel) and *ScURA3* (right panel) are indicated by arrows.

adjustment for multiple testing. Values of  $P < 0.05$  were taken to indicate significance.

## Results

*Azole stress up-regulates the genes involved in sterol uptake and biosynthesis.* Ergosterol biosynthetic genes encode the enzymes in the sterol synthetic pathway leading to ergosterol biosynthesis in yeast. It is of interest to understand whether the inhibition of ergosterol biosynthesis by azoles alters endogenous sterol synthesis in *C. glabrata* through changes in the expression of ergosterol biosynthetic genes. We found that mRNA levels of *CgERG2*, *CgERG3*, *CgERG4*, *CgERG10*, and *CgERG11* were strikingly increased in *C. glabrata* following fluconazole treatment. As seen in Table III, the extent of inducible up-regulation of *ERG* gene expression by fluconazole in these cells ranged from more than 5-fold in *CgERG3* to 19-fold in *CgERG10* compared with the untreated controls. Interestingly, we also showed a 3.7-fold increase in mRNA expression of *CgPDR16* in fluconazole-treated *C. glabrata* cells (Table III); *PDR16p* is an ATP-binding cassette (ABC)

transporter involved in the sterol biosynthetic process and phospholipid transport in *S. cerevisiae* (16).

*AUS1* and *UPC2* (or its paralog *ECM22*) have been demonstrated to be responsible for sterol uptake in *S. cerevisiae* (17). We next addressed whether inhibition of sterol synthesis by azoles alters the expression of these genes in *C. glabrata*. Sequencing data have shown that *C. glabrata* is more closely related to *Saccharomyces cerevisiae* than to *C. albicans*, and some genes are functionally exchangeable between *C. glabrata* and *S. cerevisiae*. Therefore, to identify *AUS1* and *ECM22/UPC2* orthologs in *C. glabrata*, we selected the *S. cerevisiae AUS1*, *ECM22*, and *UPC2* genes as queries to perform homology searches. A BLAST search against the *C. glabrata* open reading frame (ORF) nucleotide and amino acid sequences (www.candidagenome.org) predicted CAGLOF01419g (*CgAUS1*) to be the ortholog of *AUS1*. We also performed a BLAST search against *C. glabrata* ORF nucleotide sequence alone, which predicted CAGLOC01199g and CAGLOF07865g to be possible orthologs of *ECM22* or *UPC2*. The amino acid sequences encoded by these two genes are particularly highly homologous to *Upc2p* or *Ecm22p*. We refer

to CAGL0C01199g and CAGL0F07865g as *UPC2A* (*ECM22*) and *UPC2B* (*ECM22*), respectively. This is in concordance with the work of Nagi *et al* (4) and Whaley *et al* (18). Our results demonstrate a transcriptional up-regulation of over two-fold and over four-fold in *CgAUS1* and *CgUPC2A* expression, respectively, in our model following fluconazole challenge (Table III). These data clearly show that inhibition of ergosterol synthesis by azoles induce the expression of sterol transporter genes and likely lead to enhanced sterol uptake in *C. glabrata*.

Besides its role in anaerobic sterol uptake, *UPC2* has been shown to be an activator of ergosterol biosynthetic genes in yeast (4,18). As the up-regulation of *CgUPC2* expression was induced by fluconazole in *C. glabrata*, this result prompted us to address whether azoles alter the expression of other genes encoding transactivators responsible for sterol synthesis or uptake in fungi. It has been demonstrated that *SUT1* is a transcription factor involved in sterol uptake and synthesis in aerobically growing *S. cerevisiae* cells (19). Therefore, to identify *SUT1* ortholog in *C. glabrata*, we selected the *S. cerevisiae* *SUT1* gene as queries to perform homology searches. A BLAST search against the *C. glabrata* ORF nucleotide sequence (www.candidagenome.org) predicted CAGL0I04246g and CAGL0L09383g to be possible orthologs of *SUT1*. The amino acid sequences encoded by these two genes are particularly highly homologous to Sut1p. We refer to CAGL0I04246g and CAGL0L09383g as *CgSUT1* and *CgSUT2*, respectively. In the current model, we show that the expression of *CgSUT1*, but not *CgSUT2*, was significantly increased by fluconazole in *C. glabrata* (Table III).

*Up-regulated expression of the genes involved in sterol uptake and biosynthesis in Candida glabrata erg1 mutant.* To further assess whether ergosterol depletion affects the genes involved in sterol uptake and sterol synthesis in *C. glabrata*, we used DNA microarray to analyze gene expression in a *C. glabrata erg1* mutant with defective ergosterol biosynthesis. Transcriptional profiling of the microarrays revealed 35 genes up-regulated and 4 genes down-regulated in the *C. glabrata erg1* mutant CgTn201S compared to the parental wild-type strain Cg1660. Particularly, *C. glabrata erg1* mutant had 2.5-fold up-regulation of *CgAUS1* mRNA, 5.6-fold up-regulation of *CgTIR3* mRNA, and 3.5-fold up-regulation of *CgUPC2B* mRNA over the wild-type cells (Fig. 2). To a lesser extent, we also found that the up-regulation of *CgERG2*, *CgERG3*, *CgERG5*, *CgERG6*, *CgERG7*, *CgERG10*, *CgERG11*, and *CgERG29* in the *C. glabrata erg1* mutant cells ranged from 1.5- to 2.8-fold mRNA expression among these genes (Table IV), which is similar to our data from the *C. glabrata* cells in which ergosterol synthesis was inhibited by fluconazole (Table III). Additionally, we show a 3-fold increase in mRNA expression of *HESI/KESI*, which is involved in ergosterol biosynthesis, oxysterol binding, and sterol transport (Table IV). These data highlight the notion that blocking ergosterol synthetic pathway leading to ergosterol depletion causes increased sterol uptake activity and sterol biosynthesis in *C. glabrata*.

Besides the genes for sterol uptake and synthesis, 23 other genes demonstrated dominant and reproducible expression in *C. glabrata erg1* mutant with the average level of the six microarrays ranging from 1.5-fold to 6.3-fold greater than the wild-type strain (Table IV). These differentially expressed

Table III. Upregulated expression of sterol biosynthetic and sterol transporter genes in *Candida glabrata* under fluconazole stress.

Gene	mRNA levels
<i>ERG2</i>	11.79 <sup>a</sup>
<i>ERG3</i>	5.04 <sup>a</sup>
<i>ERG4</i>	11.08 <sup>a</sup>
<i>ERG10</i>	19.07 <sup>a</sup>
<i>ERG11</i>	5.87 <sup>a</sup>
<i>PDR16</i>	3.73 <sup>a</sup>
<i>AUS1</i>	2.51 <sup>b</sup>
<i>SUT1</i>	2.60 <sup>b</sup>
<i>SUT2</i>	0.97
<i>UPC2A</i>	4.71 <sup>a</sup>
<i>UPC2B</i>	1.60 <sup>b</sup>

Values indicate the fold-change in RNA transcription for each gene in 200  $\mu$ g/ml fluconazole-treated *C. glabrata* after normalization to RDN5.8 as the reference, as compared with the level in untreated cells, which was set as 1. <sup>b</sup>P<0.05 or <sup>a</sup>P<0.01 between fluconazole-treated and untreated *C. glabrata* cells for all values shown in this table.

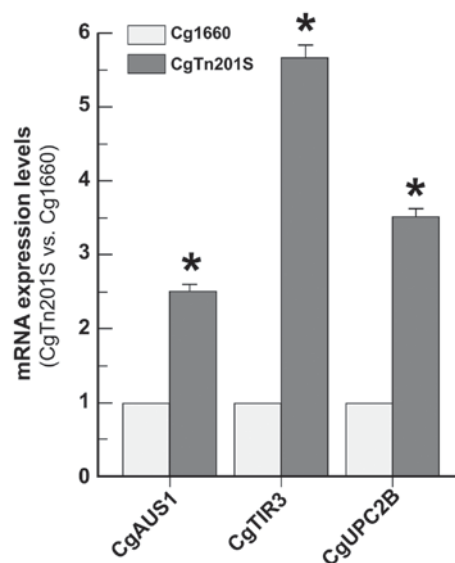


Figure 2. Expression of *CgAUS1*, *CgTIR3*, and *CgUPC2B* is up-regulated in *Candida glabrata erg1* mutant. DNA microarray was used to analyze gene expression in the *C. glabrata erg1* mutant CgTn201S and its parental wild-type strain Cg1660 as described in Materials and methods. Six microarrays were performed for analysis of the *Cgerg1* mutant/wild-type pair, including two with reciprocal labeling. The average mRNA expression levels were based on mean of six replicates. Transcriptional profiling of the microarrays revealed the up-regulation (fold-change) of *CgAUS1*, *CgTIR3*, and *CgUPC2B* in CgTn201S (*Cgerg1*) as compared with Cg1660 (wild-type), which was set as 1. <sup>a</sup>P<0.01 between the *C. glabrata erg1* mutant CgTn201S and its parental wild-type strain Cg1660 using Student's t-test.

genes were associated with multiple different cellular metabolisms and biological processes, such as iron, amino acid, and carbohydrate metabolisms, alcohol metabolism, reactive oxygen species (ROS) metabolism, heme biosynthesis, biotin biosynthesis, mitochondrion organization, mitochondrial electron

Table IV. *Candida glabrata* genes up- and down-regulated  $\geq 1.5$ -fold in response to *CgERG1* disruption (*Cgerg1* mutation) in Cg1660 host.

<i>C. glabrata</i> designation	<i>S. cerevisiae</i> homologue	Description	Fold expression <sup>a</sup>
Upregulated genes			
CAGL0F01419g	AUS1	ATP-binding cassette transporter involved in sterol uptake	2.5006
CAGL0C03872g	TIR3/YIL011w	Putative GPI-linked cell wall protein involved in sterol uptake	5.6547
CAGL0F07865g	UPC2B	Transcription factor transcriptionally regulates ergosterol biosynthetic genes and sterol transporter genes	3.4979
CAGL0L10714g	ERG2	C-8 sterol isomerase participates in ergosterol biosynthesis	2.0136
CAGL0F01793g	ERG3	C-5 sterol desaturase participates in ergosterol biosynthesis	2.7363
CAGL0M07656g	ERG5	C-22 sterol desaturase participates in ergosterol biosynthesis	2.3415
CAGL0H04653g	ERG6	C-24 sterol methyltransferase participates in ergosterol biosynthesis	2.1176
CAGL0J10824g	ERG7	Lanosterol synthase participates in ergosterol biosynthesis	2.31
CAGL0L12364g	ERG10/POT14	Acetyl-CoA C-acetyltransferase participates in ergosterol biosynthesis	2.2113
CAGL0E04334g	ERG11	Lanosterol 14- $\alpha$ -demethylase involved in ergosterol biosynthesis	2.8477
CAGL0K03927g	ERG29	Roles in ergosterol biosynthesis, mitochondrion organization, etc	1.5044
CAGL0J03916g	HES1/KES1	Roles in ergosterol biosynthesis, oxysterol binding, sterol transport, etc	2.9779
CAGL0J00297g	YHR045w	Possible roles in iron, amino acid, and carbohydrate metabolisms	1.5889
CAGL0A01089g	YPL272c	Alcohol O-acetyltransferase with role in alcohol metabolic process	4.0299
CAGL0I01408g	CYC1	Cytochrome- <i>c</i> isoform 1 involved in mitochondrial electron transport	2.6164
CAGL0L03828g	CYB5	Cytochrome b5 involved in oxidation-reduction process	1.5483
CAGL0K10868g	CTA1	Catalase A involved in cellular response to oxidative stress	2.7464
CAGL0K12100g	HEM13	Coproporphyrinogen III oxidase involved in heme biosynthesis	2.3296
CAGL0G03905g	ISA1	Regulation of ROS metabolic process and biotin biosynthetic process	1.5708
CAGL0H04851g	PPZ1	Protein phosphatase Z involved in cation homeostasis and cell wall integrity	1.633
CAGL0L07480g	NRG1/NRG2	Transcription factor activity, sequence-specific DNA binding activity	1.613
CAGL0F01485g	TIR4	Putative GPI-linked cell wall mannoprotein of the Srp1p/Tip1p family	5.4181
CAGL0H09614g	TIR1	Putative GPI-linked cell wall protein	6.3371
CAGL0C00110g	FLO1	Member of the FLO family of cell wall flocculation proteins	1.9697
CAGL0M04125g	YNL320w	Roles in cell polarity, endoplasmic reticulum, mitochondrion, etc	1.5089

Table IV. Continued.

<i>C. glabrata</i> designation	<i>S. cerevisiae</i> homologue	Description	Fold expression <sup>a</sup>
CAGL0E00187g	YMR317w	Putative adhesin-like protein; belongs to adhesin cluster IV	4.3814
CAGL0G04499g	SET4/YJL105w	Ortholog of <i>S. cerevisiae</i> : SET4 and YJL105w	1.9778
CAGL0F08965g	MSC7/YHR039c	Roles in cytosol, endoplasmic reticulum, nucleus localization, etc	1.6906
CAGL0C00209g	DAN1/YJR151c	Putative adhesin-like cell wall protein; predicted GPI-anchor	4.6475
CAGL0G10175g	DAN1/YJR151c	Adhesin-like protein; predicted GPI anchor	4.7887
CAGL0K04279g	SCM4/YGR049w	Ortholog(s) have mitochondrial outer membrane localization	1.5542
Downregulated genes			
CAGL0H03971g	YCP4/PST2	Roles in cellular response to oxidative stress, mitochondrion, etc	1.5484
CAGL0M05995g	PET10	Roles in lipid metabolism, respiratory growth, and ATP/ADP exchange	1.5975
CAGL0G05566g	FMP45	In mitochondria; role in ascospore formation, cellular response to drug, etc	1.5862
CAGL0L10142g	RSB1/YOR049c	Sphingolipid transporter; involved in fatty acid transport	2.1631

<sup>a</sup>The *Candida glabrata erg1* mutant CgTn201S vs. the parental wild-type Cg1660.

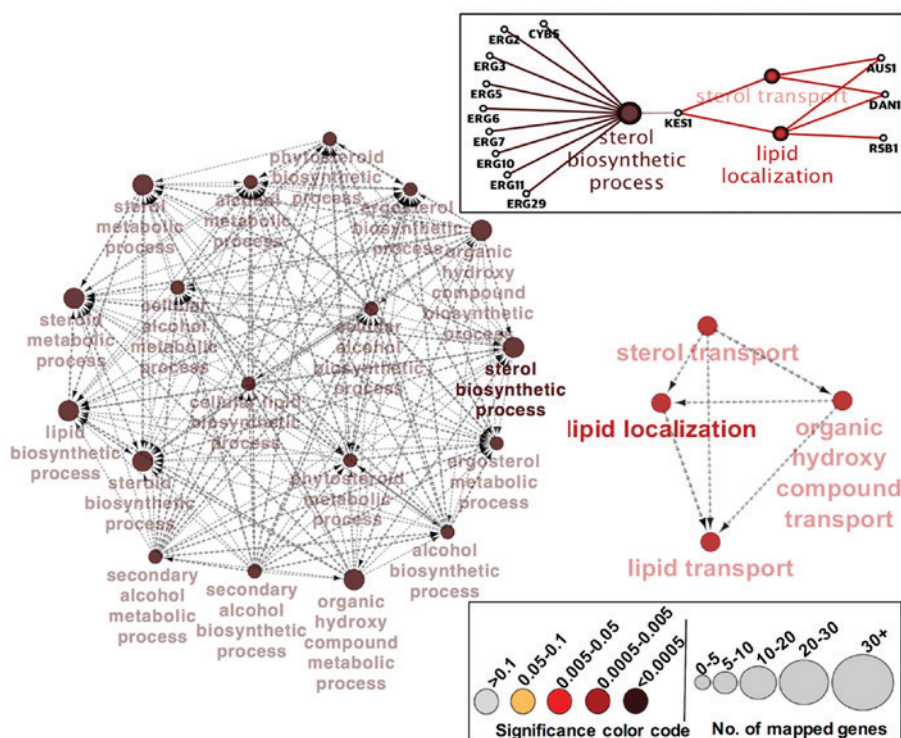


Figure 3. Two major functional networks obtained from the 35 differentially expressed genes in *Candida glabrata erg1* mutant using Cytoscape software. Each node (filled circle) represents a biological process and the size and color code indicate, respectively, the number of genes mapped and the significance of the terms (lower right inset). The direction of the network is shown by arrow-head of edges; the edge-thickness is based on kappa-score level calculated automatically by ClueGO. The molecular interaction network between the 'sterol biosynthetic process' and 'lipid localization' in combination with 'sterol transport' is shown in the upper right inset.

Table V. Functional enrichment with associated genes identified by using Cytoscape and GO database.

Enriched process	Associated gene	P-value
Sterol biosynthetic process	<i>CYB5, ERG2, ERG3, ERG5, ERG6, ERG7, ERG10, ERG11, ERG29</i>	<0.0005
Lipid localization	<i>AUS1, DAN1, RSBI</i>	0.0005 to 0.005

GO, Gene Ontology.

transport, oxidation-reduction process, cation homeostasis, cell wall integrity, and in-cell polarity, endoplasmic reticulum, mitochondrion, nucleus localization, and so forth (Table IV). Furthermore, mRNA expression of 4 genes was down-regulated 1.5- to 2.2-fold lower than the parental wild-type cells (Table IV). These down-regulated genes were enriched in several cellular and metabolic processes, including lipid metabolism, sphingolipid and fatty acid transport, respiratory growth, ATP/ADP exchange, and cellular response to oxidative stress (Table IV).

*Potential coordination between sterol biosynthesis and sterol uptake in Candida glabrata erg1 mutant.* To further explore the functional themes of the above 35 differentially expressed genes in *C. glabrata erg1* mutant, we used Cytoscape, a bioinformatics software for visualizing functional and molecular interaction networks. The functional interaction networks in Fig. 3 support our interpretation that the ergosterol biosynthetic process is the major biological function affected in *C. glabrata* mutant strain lacking *ERG1*. To compensate for the defective sterol biosynthetic pathway in the cell, and overcome the imbalance in cellular levels of sterol, cells increase the sterol uptake machinery and ergosterol biosynthesis processes in order to survive under azole and environmental stress. As shown in Fig. 3, nine genes (*ERG2, ERG3, ERG5, ERG6, ERG7, ERG10, ERG11, ERG29, and CYB5*) comprise the largest network cluster and contribute towards the enrichment of the ‘sterol biosynthetic process.’ While three genes (*AUS1, DAN1, and RSBI*) in the other smaller functional network cluster are enriched with ‘lipid localization’ in combination with GO-term ‘sterol transport’ (Fig. 3). *KES1* and *HES1* are the genes bridging the two major clusters by establishing a potential coordination between the ‘sterol biosynthetic process’ and ‘lipid localization/sterol transport’ (Fig. 3). The enriched processes identified with the Cytoscape software and GO database using the differentially expressed genes in *C. glabrata erg1* mutant are shown in Table V.

*Candida glabrata aus1* deletant is defective in sterol uptake and has greater susceptibility to azoles under hypoxic conditions. Lastly, we validated whether *C. glabrata* cells accumulate sterols from the environment through the Aus1p transporter and whether sterol uptake confers resistance to azoles in *C. glabrata*. To distinguish the uptake of exogenous sterol from that of endogenous ergosterol biosynthesis, we generated a *C. glabrata erg1/aus1Δ* double mutant strain and used the *C. glabrata erg1* mutant strain CgTn201S and the wild-type strain Cg1660 as the controls. As seen in

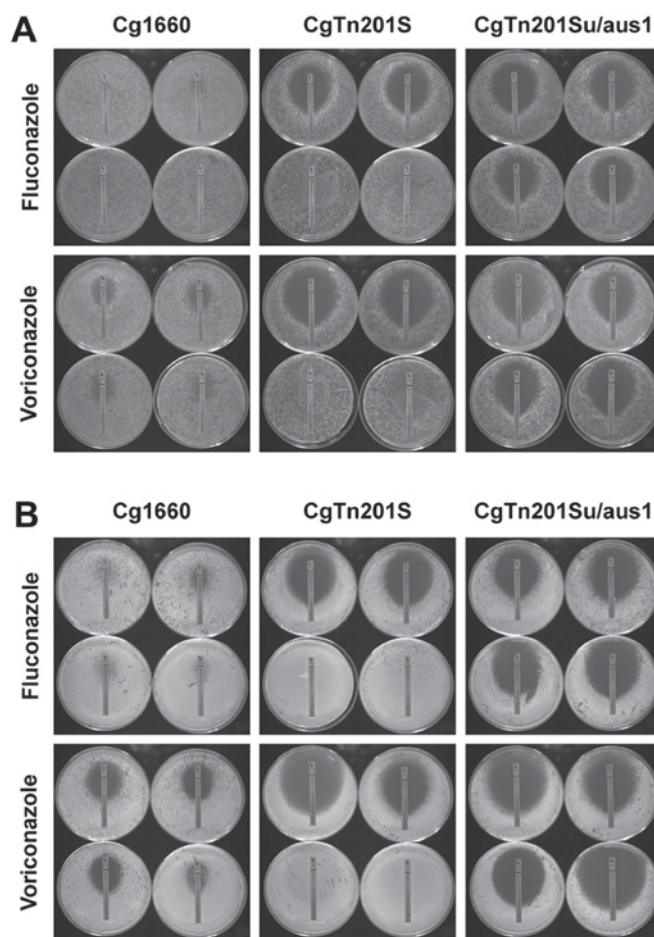


Figure 4. *CgAUS1* deletion in *Candida glabrata* abolishes the effect of sterol supplement on azole susceptibility under hypoxic conditions. Cg1660 (wild-type), CgTn201S (*Cgerg1*), or CgTn201Su/*aus1* (*Cgerg1/aus1Δ*) were grown on (A) MIN agar medium or (B) YEPG agar medium. Plates were incubated under conditions of low oxygen tension at 37°C for 3 days. The fluconazole and voriconazole susceptibilities of Cg1660, CgTn201S, and CgTn201Su/*aus1* were analyzed by E-test. The intercept of the zone of growth inhibition with the paper strip indicates the minimum inhibitory concentration (MIC). The addition of cholesterol or ergosterol is indicated by the position within each of the four groups as follows: upper left corner, MIN or YEPG; upper right corner, MIN or YEPG with ethanol-Tween 80 solvent alone; lower left corner, MIN or YEPG with cholesterol; and lower right corner, MIN or YEPG with ergosterol. The numerical data are shown in Tables VI and VII for MIN agar cultures and YEPG agar cultures, respectively.

Fig. 4A and B and Tables VI and VII, in the presence of exogenous cholesterol or ergosterol, *C. glabrata erg1* mutant cells showed much lower susceptibility to fluconazole and voriconazole compared to those cells in the absence of exogenous sterols, suggesting that *C. glabrata erg1* mutant cells are

Table VI. Inhibitory effect of azoles in *Candida glabrata* wild-type, *erg1* mutant, and *erg1/aus1Δ* double mutant on MIN agar medium with sterol supplement under hypoxic condition.

Strain <sup>a</sup>	E-test on MIN agar medium				
	Detergent (0.5% EtOH and 0.5% Tween-80)	Cholesterol (20 μg/ml)	Ergosterol (20 μg/ml)	Fluconazole MIC (μg/ml)	Voriconazole MIC (μg/ml)
Cg1660	-	-	-	>256	4.0
Cg1660	+	-	-	>256	4.0
Cg1660	+	+	-	>256	12
Cg1660	+	-	+	>256	12
CgTn201S	-	-	-	0.50	0.064
CgTn201S	+	-	-	0.50	0.064
CgTn201S	+	+	-	>256	>32
CgTn201S	+	-	+	>256	>32
CgTn201Su/Cgaus1	-	-	-	0.50	0.064
CgTn201Su/Cgaus1	+	-	-	0.50	0.064
CgTn201Su/Cgaus1	+	+	-	0.50	0.064
CgTn201Su/Cgaus1	+	-	+	0.50	0.064

<sup>a</sup>Under hypoxic conditions (1% O<sub>2</sub>). Cg1660, *C. glabrata* wild-type; CgTn201S, *C. glabrata erg1* mutant; CgTn201S/Cgaus1, *C. glabrata erg1/aus1Δ* double mutant; EtOH, ethanol; MIC, minimum inhibitory concentration.

Table VII. Inhibitory effect of azoles in *Candida glabrata* wild-type, *erg1* mutant, and *erg1/aus1Δ* double mutant on YEPG agar medium with sterol supplement under hypoxic condition.

Strain <sup>a</sup>	E-test on YEPG agar medium				
	Detergent (0.5% EtOH and 0.5% Tween-80)	Cholesterol (20 μg/ml)	Ergosterol (20 μg/ml)	Fluconazole MIC (μg/ml)	Voriconazole MIC (μg/ml)
Cg1660	-	-	-	>256	1.0
Cg1660	+	-	-	>256	1.0
Cg1660	+	+	-	>256	1.0
Cg1660	+	-	+	>256	6.0
CgTn201S	-	-	-	1.0	0.064
CgTn201S	+	-	-	1.0	0.064
CgTn201S	+	+	-	>256	>32
CgTn201S	+	-	+	>256	>32
CgTn201Su/Cgaus1	-	-	-	1.0	0.064
CgTn201Su/Cgaus1	+	-	-	1.0	0.064
CgTn201Su/Cgaus1	+	+	-	1.0	0.064
CgTn201Su/Cgaus1	+	-	+	1.0	0.064

<sup>a</sup>Under hypoxic conditions (1% O<sub>2</sub>). Cg1660, *C. glabrata* wild-type; CgTn201S, *C. glabrata erg1* mutant; CgTn201S/Cgaus1, *C. glabrata erg1/aus1Δ* double mutant; EtOH, ethanol; MIC, minimum inhibitory concentration.

capable of accumulating sterols from the medium through the wild-type sterol transporter CgAus1p; but not through ergosterol synthesis because the cells were defective in ergosterol synthetic pathway. In contrast, in the presence of exogenous cholesterol or ergosterol, the *C. glabrata erg1/aus1Δ* double mutant shows much higher susceptibility to fluconazole and voriconazole than the *C. glabrata erg1* mutant, indicating that *C. glabrata erg1/aus1Δ* double mutant cells are not able to uptake and synthesize sterols due to defective conditions in both the CgAus1p transporter and ergosterol biosynthesis

in the cells. We also tested whether the loss of CgAus1p in *C. glabrata* sensitizes the pathogen to polyene amphotericin B and the echinocandins anidulafungin and caspofungin, and our E-test results reveal that *C. glabrata* cells lacking CgAus1p do not show altered susceptibility to non-azole antifungals in the presence or absence of exogenous sterols (data not shown). These observations confirm the findings of Zavrel *et al* (20) that CgAus1p is responsible for taking up exogenous cholesterol or ergosterol in *C. glabrata* under hypoxic stress when sterol synthesis is either absent or

insufficient, and further suggest that sterol uptake plays an important role in the development of azole resistance in yeast under ergosterol starvation conditions, such as under azole drug pressure or when defective in sterol biosynthesis.

## Discussion

Yeast develops strategies to grow and survive in different unfavorable environments. In the present study, we observed that *C. glabrata* acquires two protective mechanisms to allow the pathogen to grow and survive under azole and hypoxic stress: Through increasing endogenous sterol synthesis or through importing exogenous sterols. Our data revealed that the expression of both ergosterol biosynthesis and sterol metabolism regulator genes, as well as sterol influx transporter genes, are significantly increased in *C. glabrata* under fluconazole stress. Likewise, the sterol influx transporter genes (*CgAUS1* and *CgTIR3*) and the ergosterol biosynthetic genes (*CgERG2*, *CgERG3*, *CgERG5*, *CgERG6*, *CgERG7*, *CgERG10*, *CgERG11*, and *CgERG29*) are markedly up-regulated in yeast when ergosterol biosynthesis is suppressed either under hypoxia or due to defective sterol synthesis. We also confirmed that *CgAUS1* in the cell is responsible for importing exogenous cholesterol and ergosterol, thus allowing *C. glabrata* to survive under low oxygen tension conditions or under azole pressure. The presence of both *in vivo* suggests an underlying mechanism for azole resistance in clinical practice.

Nakayama and colleagues show that *CgAUS1* protects *C. glabrata* cells against azoles in the presence of serum (21). The composition of serum is complicated, and it includes many different molecules, minerals, and nutrients other than cholesterol. It is possible that, besides importing cholesterol via the sterol transporter *CgAUS1*, *C. glabrata* cells may also take up other molecules and nutrients from serum that are necessary to their survival amidst azole treatment. In our experiments, as in those of Zavrel *et al.* (20), we did not use serum but solubilized cholesterol and ergosterol using the detergent Tween 80. This allowed for the incorporation of exogenous sterol into the fungal cell. Our results, together with the data discussed above, reinforce the understanding of how both enhanced endogenous sterol synthesis and increased exogenous sterol uptake by yeast are integral to conferring resistance to azole therapy in fungal infections. Resistance to azole treatment not only limits the usefulness of this class of drugs, it also drives the survival of intrinsically low-susceptibility *C. glabrata* cells that become increasingly resistant following prolonged treatment with azole therapeutic agents.

Combining our data in this study, we propose a hypothetical model in which sterol uptake and sterol biosynthesis act coordinately and collaboratively to mediate azole antifungal resistance in *C. glabrata* under azole and hypoxic stress as shown in Fig. 5. In this model, azole and hypoxic stresses deplete ergosterol directly or indirectly by inhibiting ergosterol biosynthesis. Hypoxia and azoles cause mitochondrial dysfunction by depriving the mitochondria of oxygen and inducing the accumulation of toxic sterol-intermediates, ultimately leading to the reduction of ergosterol biosynthesis. In response, ergosterol depletion triggers up-regulation of the genes involved in sterol transport and ergosterol biosynthesis,

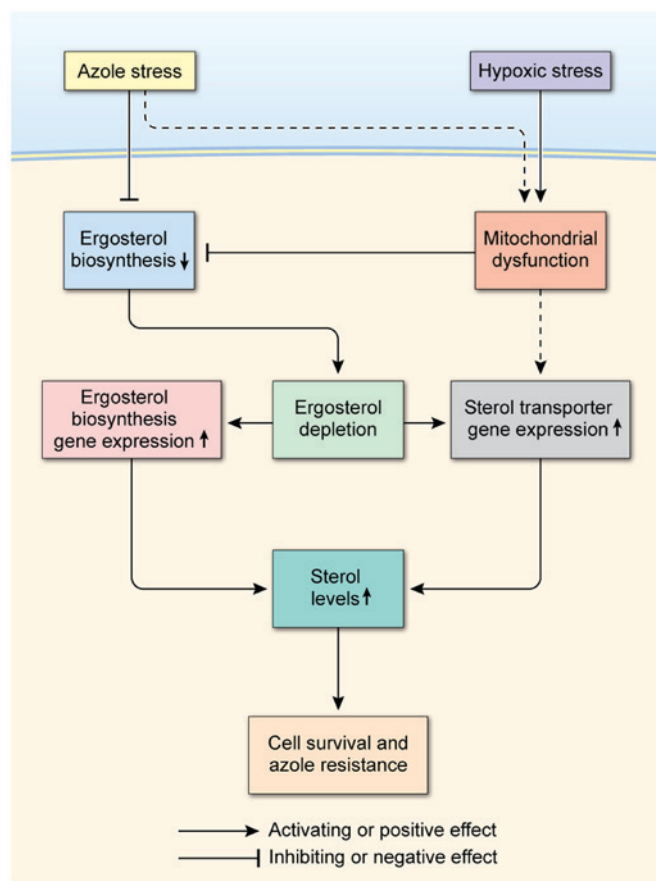


Figure 5. A schematic diagram illustrating a hypothetical model for sterol uptake and sterol biosynthesis acting coordinately and collaboratively in mediating azole antifungal resistance in *Candida glabrata* under azole and hypoxic stress. See 'Discussion' for further elaboration.

leading to increases in sterol levels. Because both sterol uptake and sterol biosynthesis increase sterol levels through distinct mechanisms, they both may function together to maintain sterol levels and sustain cell growth. Such a cooperative mechanism may serve to integrate the roles of sterol transport and sterol biosynthesis culminating in cell survival, which may underlie the mechanism of azole antifungal resistance in *C. glabrata*.

Collectively, this study shows the up-regulation of the genes involved in ergosterol biosynthesis and sterol transport in *C. glabrata* cells in which sterol synthesis is defective or is abrogated by fluconazole treatment. We also corroborate that the sterol influx transporter *CgAUS1* imports exogenous cholesterol or ergosterol, which contributes to the development of clinical resistance to azole antifungals in *C. glabrata*. These findings demonstrate that sterol uptake and sterol biosynthesis may act coordinately and collaboratively to sustain growth and to mediate antifungal resistance in *C. glabrata* through dynamic gene expression in response to azole stress and environmental challenges.

## Acknowledgements

The authors would like to thank Ms. Cindy Clark for carefully reviewing the manuscript.

## Funding

This study was supported by the Intramural Research Program of the National Institute of Allergy and Infectious Diseases, National Institutes of Health.

## Availability of data and materials

All data generated or analyzed during this study are included in this published article.

## Authors' contributions

QQL conceived of the project, conducted the studies, performed drug sensitivity assay, RT-qPCR and Southern blot analysis, cloning of *CgAUS1*, construction of *Cgerg1* and *Cgaus1* double mutant, as well as other experiments, carried out the analysis and interpretation of data, wrote the manuscript, and is the primary author of this paper. HFT conceived the project, performed microarray hybridization and data analysis, and critically reviewed the manuscript. AM performed bioinformatics and statistical analysis. BAW, JAN, and YF analyzed and interpreted data and edited the manuscript. JEB participated in the design and coordination of the study, critically reviewed the manuscript, and edited the final version of the paper. All authors read and approved the final manuscript.

## Ethics approval and consent to participate

Not applicable.

## Consent for publication

Not applicable.

## Competing interests

The authors declare that they have no competing interests.

## References

- Pappas PG, Kauffman CA, Andes DR, Clancy CJ, Marr KA, Ostrosky-Zeichner L, Reboli AC, Schuster MG, Vazquez JA, Walsh TJ, *et al*: Executive summary: Clinical practice guideline for the management of candidiasis: 2016 update by the infectious diseases society of America. *Clin Infect Dis* 62: 409-417, 2016.
- Rodrigues CF, Silva S and Henriques M: *Candida glabrata*: A review of its features and resistance. *Eur J Clin Microbiol Infect Dis* 33: 673-688, 2014.
- Inukai T, Nagi M, Morita A, Tanabe K, Aoyama T, Miyazaki Y, Bard M and Nakayama H: The mannoprotein TIR3 (CAGL0C03872g) is required for sterol uptake in *Candida glabrata*. *Biochim Biophys Acta* 1851: 141-151, 2015.
- Nagi M, Nakayama H, Tanabe K, Bard M, Aoyama T, Okano M, Higashi S, Ueno K, Chibana H, Niimi M, *et al*: Transcription factors CgUPC2A and CgUPC2B regulate ergosterol biosynthetic genes in *Candida glabrata*. *Genes Cells* 16: 80-89, 2011.
- Nagi M, Tanabe K, Ueno K, Nakayama H, Aoyama T, Chibana H, Yamagoe S, Umeyama T, Oura T, Ohno H, *et al*: The *Candida glabrata* sterol scavenging mechanism, mediated by the ATP-binding cassette transporter Aus1p, is regulated by iron limitation. *Mol Microbiol* 88: 371-381, 2013.
- Silver PM, Oliver BG and White TC: Role of *Candida albicans* transcription factor Upc2p in drug resistance and sterol metabolism. *Eukaryot Cell* 3: 1391-1397, 2004.
- MacPherson S, Akache B, Weber S, De Deken X, Raymond M and Turcotte B: *Candida albicans* zinc cluster protein Upc2p confers resistance to antifungal drugs and is an activator of ergosterol biosynthetic genes. *Antimicrob Agents Chemother* 49: 1745-1752, 2005.
- Tsai HF, Bard M, Izumikawa K, Krol AA, Sturm AM, Culbertson NT, Pierson CA and Bennett JE: *Candida glabrata* *erg1* mutant with increased sensitivity to azoles and to low oxygen tension. *Antimicrob Agents Chemother* 48: 2483-2489, 2004.
- Bard M, Sturm AM, Pierson CA, Brown S, Rogers KM, Nabinger S, Eckstein J, Barbuch R, Lees ND, Howell SA and Hazen KC: Sterol uptake in *Candida glabrata*: Rescue of sterol auxotrophic strains. *Diagn Microbiol Infect Dis* 52: 285-293, 2005.
- Flowers SA, Colón B, Whaley SG, Schuler MA and Rogers PD: Contribution of clinically derived mutations in ERG11 to azole resistance in *Candida albicans*. *Antimicrob Agents Chemother* 59: 450-460, 2015.
- Li QQ, Skinner J and Bennett JE: Evaluation of reference genes for real-time quantitative PCR studies in *Candida glabrata* following azole treatment. *BMC Mol Biol* 13: 22, 2012.
- Vermitsky JP, Earhart KD, Smith WL, Homayouni R, Edlind TD and Rogers PD: Pdr1 regulates multidrug resistance in *Candida glabrata*: Gene disruption and genome-wide expression studies. *Mol Microbiol* 61: 704-722, 2006.
- Shannon P, Markiel A, Ozier O, Baliga NS, Wang JT, Ramage D, Amin N, Schwikowski B and Ideker T: Cytoscape: A software environment for integrated models of biomolecular interaction networks. *Genome Res* 13: 2498-2504, 2003.
- Bindea G, Mlecnik B, Hackl H, Charoentong P, Tosolini M, Kirilovsky A, Fridman WH, Pages F, Trajanoski Z and Galon J: ClueGO: A Cytoscape plug-in to decipher functionally grouped gene ontology and pathway annotation networks. *Bioinformatics* 25: 1091-1093, 2009.
- Bindea G, Galon J and Mlecnik B: CluePedia Cytoscape plugin: Pathway insights using integrated experimental and in silico data. *Bioinformatics* 29: 661-663, 2013.
- van den Hazel HB, Pichler H, do Valle Matta MA, Leitner E, Goffeau A and Daum G: PDR16 and PDR17, two homologous genes of *Saccharomyces cerevisiae*, affect lipid biosynthesis and resistance to multiple drugs. *J Biol Chem* 274: 1934-1941, 1999.
- Marek M, Milles S, Schreiber G, Daleke DL, Dittmar G, Herrmann A, Müller P and Pomorski TG: The yeast plasma membrane ATP binding cassette (ABC) transporter Aus1: Purification, characterization, and the effect of lipids on its activity. *J Biol Chem* 286: 21835-21843, 2011.
- Whaley SG, Caudle KE, Vermitsky JP, Chadwick SG, Toner G, Barker KS, Gygyax SE and Rogers PD: UPC2A is required for high-level azole antifungal resistance in *Candida glabrata*. *Antimicrob Agents Chemother* 58: 4543-4554, 2014.
- Ness F, Bourrot S, Régnacq M, Spagnoli R, Bergès T and Karst F: SUT1 is a putative Zn[II]2Cys6-transcription factor whose upregulation enhances both sterol uptake and synthesis in aerobically growing *Saccharomyces cerevisiae* cells. *Eur J Biochem* 268: 1585-1595, 2001.
- Zavrel M, Hoot SJ and White TC: Comparison of sterol import under aerobic and anaerobic conditions in three fungal species, *Candida albicans*, *Candida glabrata*, and *Saccharomyces cerevisiae*. *Eukaryot Cell* 12: 725-738, 2013.
- Nakayama H, Tanabe K, Bard M, Hodgson W, Wu S, Takemori D, Aoyama T, Kumaraswami NS, Metzler L, Takano Y, *et al*: The *Candida glabrata* putative sterol transporter gene CgAUS1 protects cells against azoles in the presence of serum. *J Antimicrob Chemother* 60: 1264-1272, 2007.



This work is licensed under a Creative Commons Attribution-NonCommercial-NoDerivatives 4.0 International (CC BY-NC-ND 4.0) License.